Materials Science in Semiconductor Processing 24 (2014) 157–163

Contents lists available at ScienceDirect

Materials Science in Semiconductor Processing

journal homepage: www.elsevier.com/locate/mssp

The effects of Dea:water ratio on the properties of ZnO nanofilms obtained by spin coating method

Ümit Özlem Akkaya Arıer [a,*], Bengü Özuğur Uysal [b]

[a] Department of Physics, Mimar Sinan Fine Arts University, Sisli, Istanbul 34347, Turkey
[b] Department of Energy Systems Engineering, Faculty of Engineering and Natural Sciences, Kadir Has University, Fatih, Istanbul 34083, Turkey

ARTICLE INFO

Available online 3 April 2014

Keywords:
ZnO
Nanoparticles
Thin films
Size
Sol–gel

ABSTRACT

In this work, the ZnO were fabricated with the sol–gel spin coating method, and the effects of the Dea:water ratios on the properties of the as-prepared ZnO thin films were determined by using a X-ray diffractometer, transmission electron microscope, scanning electron microscope, atomic force microscope, ultraviolet–visible spectrophotometer, and spectrophotometer. Experimental results indicated that the Dea:water ratio affected the structural and optical properties of the ZnO films considerably. The activation energy for the particle growth of ZnO nanofilms and the effects of the Dea:water ratios on the band gap values of the ZnO films were investigated. The film has an activation energy of 26.3 kJ/mol, and optical band gap of 3.27–3.31 eV is proportional to the Dea:water ratio.

1. Introduction

Zinc oxide (ZnO) is a semiconductor material that has a wide band gap, large exciton binding energy, wide range resistivity, high mobility and high transparency [1–4]. ZnO structures usually exhibit n-type conductivity due to their defects of zinc interstitials and oxygen vacancies. They are economic, non-toxic and chemically stable metal oxide materials. ZnO structures have a number of applications in thin-film solar cells, thin film transistors, surface acoustic wave devices and sensors, solar cells and display devices [1–7]. Various growth methods have been used to prepare ZnO films such as sol–gel [7–10], chemical vapor deposition (CVD) [11–16], pulsed laser deposition (PLD) [17–20], sputtering [21–25], and molecular beam epitaxy (MBE) [26–29]. Among the above mentioned preparation techniques, the easiest and low-cost sol–gel method allows to control the structures of films. ZnO nanoparticles have been very important structures for solar energy conversion, photocatalysis, luminescence, and sensors applications in recent years [10,30,31]. The purpose of this study is controlling the structural and optical properties of nanostructured ZnO films which were deposited on glass substrates using the spin-coating method by changing Dea:water ratios. The calculated activation energy for the particle growth of ZnO nanofilms was found to be lower than the values reported in the literature. These quantitative findings in this work would be useful for the controlled synthesis and study of growth kinetics of ZnO nanoparticles for potential applications.

2. Experimental

2.1. Preparation of ZnO films

ZnO thin films were prepared using the sol–gel chemistry method. The sol was prepared by dissolving zinc acetate dehydrate (ZnAc) in 2propanol. Dea (Diethanolamine), which is a surface active material, is used to accelerate solving. Water was added for hydrolysis reactions.

* Corresponding author. Fax: +90 212 2611121.
E-mail address: oarier@msgsu.edu.tr (Ü.Ö. Akkaya Arıer).

http://dx.doi.org/10.1016/j.mssp.2014.03.033
1369-8001/

As a precursor solution of ZnAc:2propanol:Dea:water, a volume ratio of 0.4:4:0.1:0.2 was used. ZnAc, 2propanol and Dea concentrations were held fixed, and crystallite size was controlled only by changing the Dea:water volume ratio, e.g., to 16, 8, 4, and 2. These sols were mixed using magnetic stirring for 1 h at 60 °C. The obtained solution was deposited on Corning 2947 glass substrates by spin-coating deposition (1000 rpm/30 s), using a spin coater in the room temperature (21 °C). After coating, ZnO films were immediately placed in a microprocessor-controlled (CWF 1100) furnace which was already heated at 450 °C. The films were taken out of the furnace and were left at the room temperature at the end of 1 h. The thickness of ZnO films was measured to be approximately 60 nm.

2.2. Sample characterization

Structures of produced films deposited on glass substrates were characterized by X-ray diffractometer (XRD, GBC-MMA, Cu-Kα radiation). The surface morphology was characterized by a transmission electron microscope (HR-TEM), scanning electron microscope (SEM, S-3100H, Hitachi Ltd.), and atomic force microscope (AFM, Shimadzu scanning probe microscope SPM-9500J3). Optical transmittance of films was determined by a spectrophotometer (Perkin Elmer). Spectroscopic analysis of ZnO films was performed using a UV visible spectrophotometer (Agilent 8453).

3. Results and discussion

The XRD spectra of the ZnO films prepared at 450 °C for various Dea:water volume ratios are shown in Fig. 1. The films prepared at room temperature exhibit an amorphous structure while the films prepared at 400–550 °C show crystalline structure. The XRD spectrum reveals that the films have hexagonal wurtzite structure (JCPDS: 36-1451) with peaks at {1 0 0}, {0 0 2}, and {1 0 1} diffraction planes of the ZnO crystal structure. Among these diffraction peaks, the {0 0 2} diffraction located at 34.5° is the most intensive one.

The crystallite size of ZnO film is calculated according to the XRD results using the Debye–Scherrer [32] equation

$$D = \frac{K\lambda}{B\cos\theta},$$

where D is the diameter of the zincoxide nanocrystallites, K is a constant (0.89), λ is the wavelength of the incident light (for Cu Kα radiation $\lambda = 1.54056$ Å), B is the full width at half-maximum (FWHM) of the diffraction line and θ is the Bragg angle. The calculated sizes of the ZnO nanocrystallites determined from {1 0 0}, {0 0 2}, and {1 0 1} peaks are listed in Table 1. The average crystallite sizes are found to be 2.0, 4.3, 6.1, and 9.6 nm for ZnO thin film with Dea:water volume ratios of 16; 8; 4; and 2, respectively. The weakening and broadening of the XRD peaks are attributed to the decrease of the crystallite size.

The results show that when zinc acetate dehydrates, 2propanol and Dea concentrations were held fixed, the crystallite size decreased with the increasing Dea:water volume ratio. The crystallite size of films increases due to the increase in the amount of water, which causes agglomeration. Amount of water in ZnO solution affects the hydrolysis and the nucleation reactions. The hydrolysis

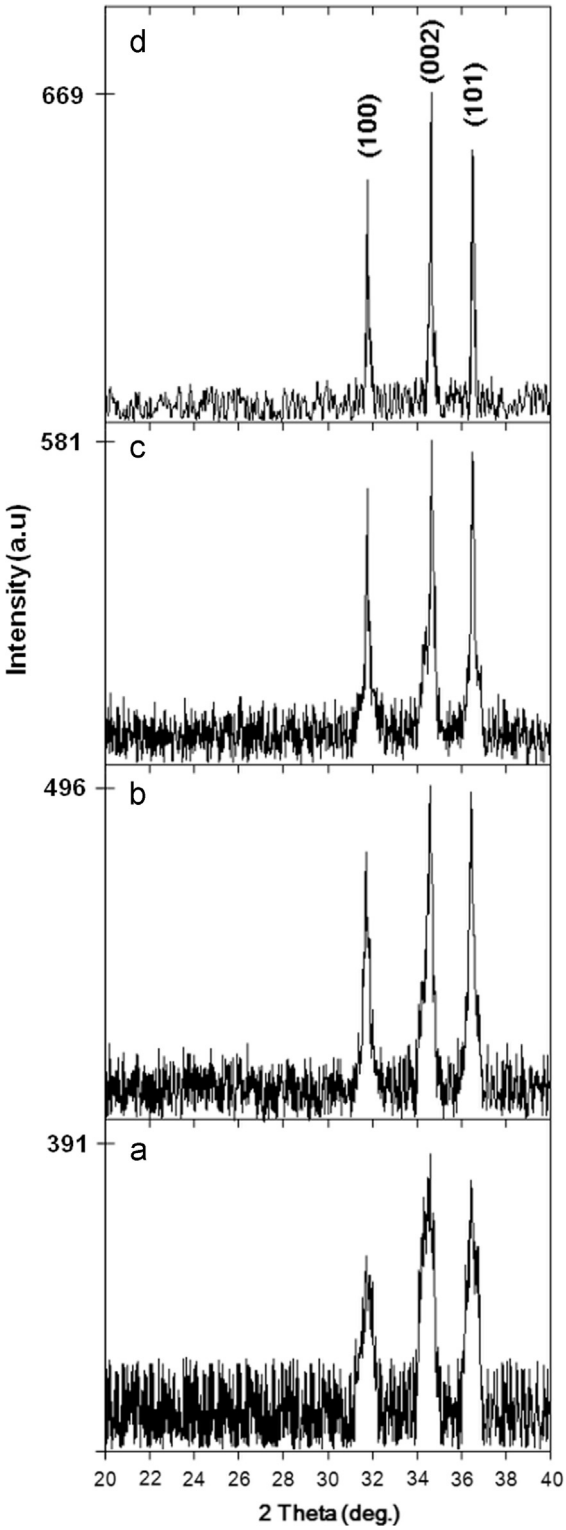

Fig. 1. X-ray diffraction patterns of ZnO nanofilms for different Dea:water volume ratios: (a) 16, (b) 8, (c) 4, and (d) 2.

Table 1
Crystallite sizes of nanostructured zincoxide thin films with different ratios of Dea:water at annealing temperature of 450 °C.

Dea: water ratio	Crystallite size for {1 0 0} diffraction plane (nm)	Crystallite size for {0 0 2} diffraction plane (nm)	Crystallite size for {1 0 1} diffraction plane (nm)
16	1.93	2.19	2
8	3.1	5.1	4.7
4	5.7	6.5	6.1
2	8.64	10.2	9.83

rates are low in the solvents for less water ratio which include too much alkoxide. When zinc acetate dehydrated, 2propanol, Dea and water concentration were fixed, the effects of the heat treatment temperature on the crystallite size of the films are investigated in Fig. 2.

The crystallite size of films increases with the increase in the heat treatment temperature due to the increased crystallization. The crystallite size-dependence and the temperature-dependence of activation energy, E can be expressed using the Arrhenius equation as

$$E = -RT \ln(d/a),$$

where T is the temperature (Kelvin), and d is the average crystallite size, a is the intercept, and R is the universal gas constant. Fig. 3 shows the activation energy for the particle growth of ZnO nanostructured film for Dea:water volume ratio of 4, which was determined as 26.3 kJ/mol using the slope of the lines of a plot of the logarithm of the crystallite size versus temperature (1000/T). Low energy is required for the particle growth of the ZnO films because of the small size particles. Similar calculations have been reported before for different ZnO nanostructures [33–35]. The growth activation energies of ZnO nanowires have been estimated to be 234 kJ/mol in the work of Yang et al. [33]. The activation energy of metal oxidation at reactions with supercritical H_2O, CO_2 and their mixtures has been calculated to be 53.23 kJ/mol using bulk zinc based on the temperature dependence of the growth rate of Zn reacting with H_2O by Vostrikov et al. [34]. Our calculated activation energy is much lower in comparison to reported values in the literature. Because, among these structures the nanoparticled thin films have a higher surface area, and less energy is required to induce the particle growth of nanostructured films.

TEM images of nanostructured ZnO which are fabricated for various Dea:water ratios at 450 °C are exhibited in Fig. 4. This result indicates that the grain size of the ZnO nanoparticles increased with the decreasing Dea: water ratio.

Fig. 5 shows the SEM images of ZnO films which are compared for various Dea:water ratios at 450 °C. The films exhibited a uniform pore distribution all over the surface, and the size of the ZnO nanoparticles in films increased with the decreasing Dea:water ratio. TEM and SEM images present the fact that the size of nanoparticles is in agreement with crystallite size, which is determined using the Debye–Scherrer formula.

The AFM images of the synthesized films for various Dea:water ratios are shown in Fig. 6. The results show that

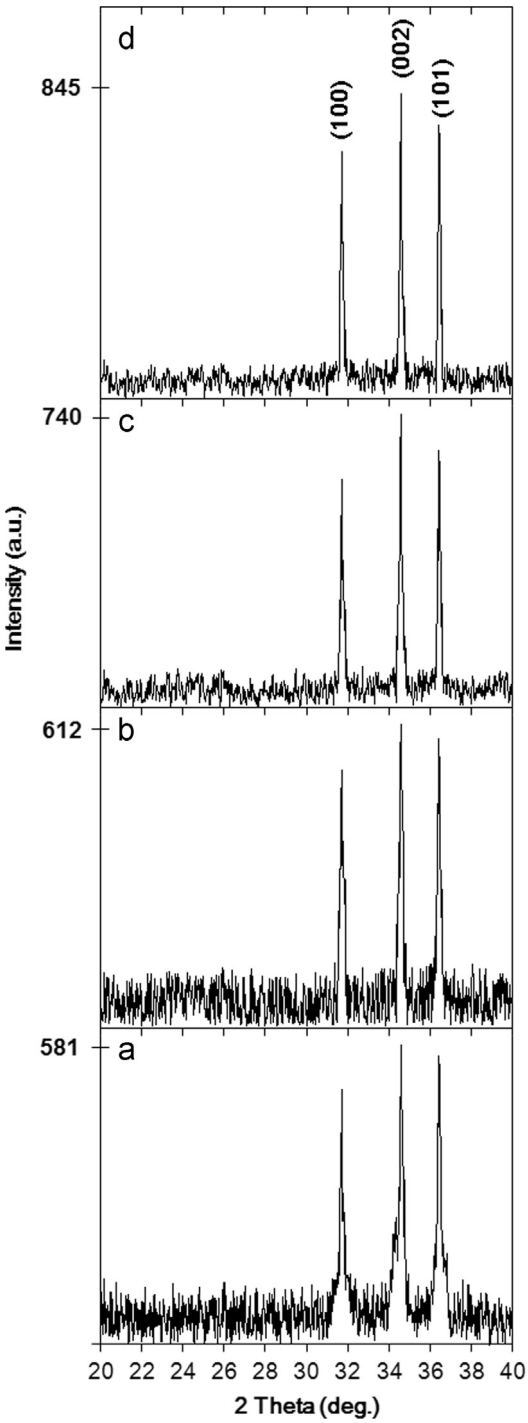

Fig. 2. X-ray diffraction patterns of ZnO nanofilms (Dea:water volume ratio:4) for different heat treatment temperatures: (a) 450, (b) 500, (c) 550, and (d) 600 °C.

the films are compact, and the nanoparticles cover the whole substrate. Surface roughness of films was determined to be Rms: 3.12; 5.23; 7.61; 9.15 nm for 16; 8; 4; 2 Dea:water ratios using AFM, respectively. The roughness of the films decreased with an increase in the Dea:water

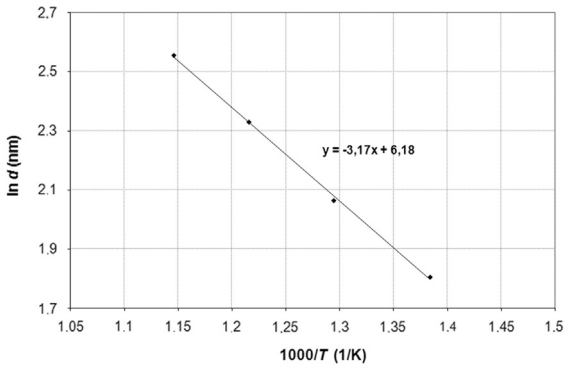

Fig. 3. Plot of ln d versus 1000/T of ZnO nanofilms (Dea:water volume ratio:4).

ratio. It is also been observed that the grain size decreased with the increase in Dea:water ratios.

Fig. 7 shows the optical absorption spectra of the synthesized ZnO nanostructured films. A red shift of the absorption band edge was observed in films with decrease in Dea:water ratio. The ZnO nanoparticles absorb visible light within a wavelength above 380 nm by decreasing the ratios. The ZnO nanoparticles cause obvious absorption edge shifts of UV–vis spectra which are sensitive to surface characteristics as a result of the increase in Dea:water ratios due to the quantum size and Burstein–Moss effects [36]. These effects are very important for ZnO nanoparticles in the films.

Fig. 8 shows that transmission values of ZnO nanostructured films is decreased with the decrease of Dea:

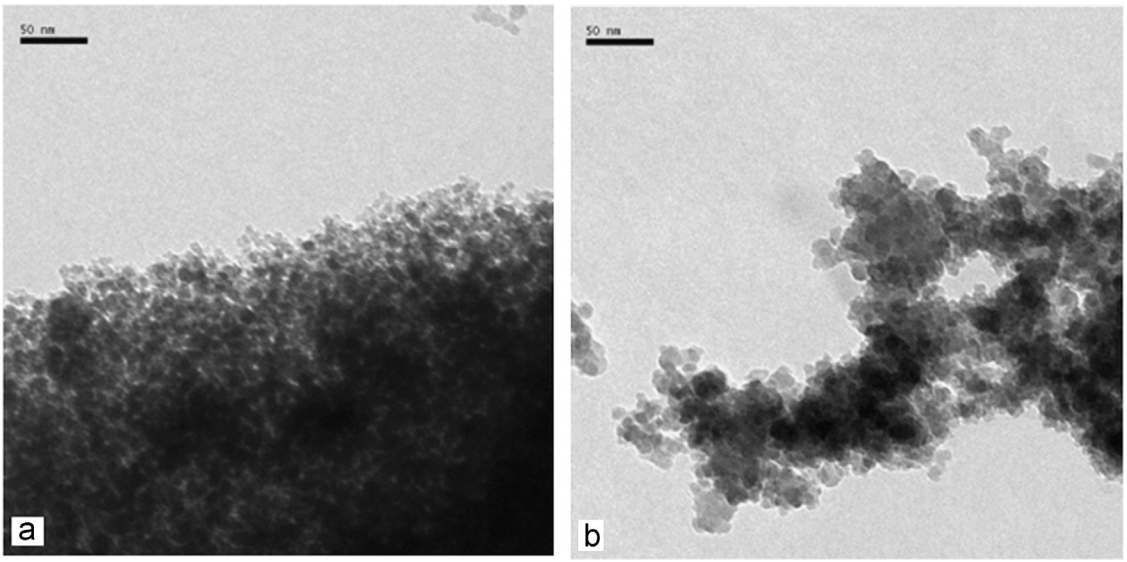

Fig. 4. TEM images of ZnO nanofilms with different Dea:water volume ratios: (a) 4 and (b) 2.

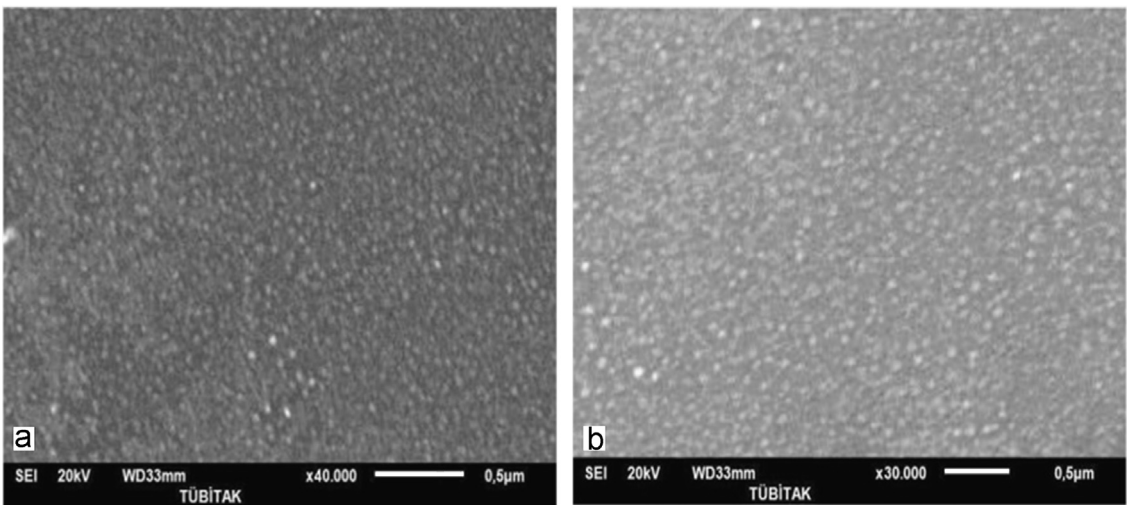

Fig. 5. SEM images of ZnO nanofilms with different Dea:water volume ratios: (a) 4 and (b) 2.

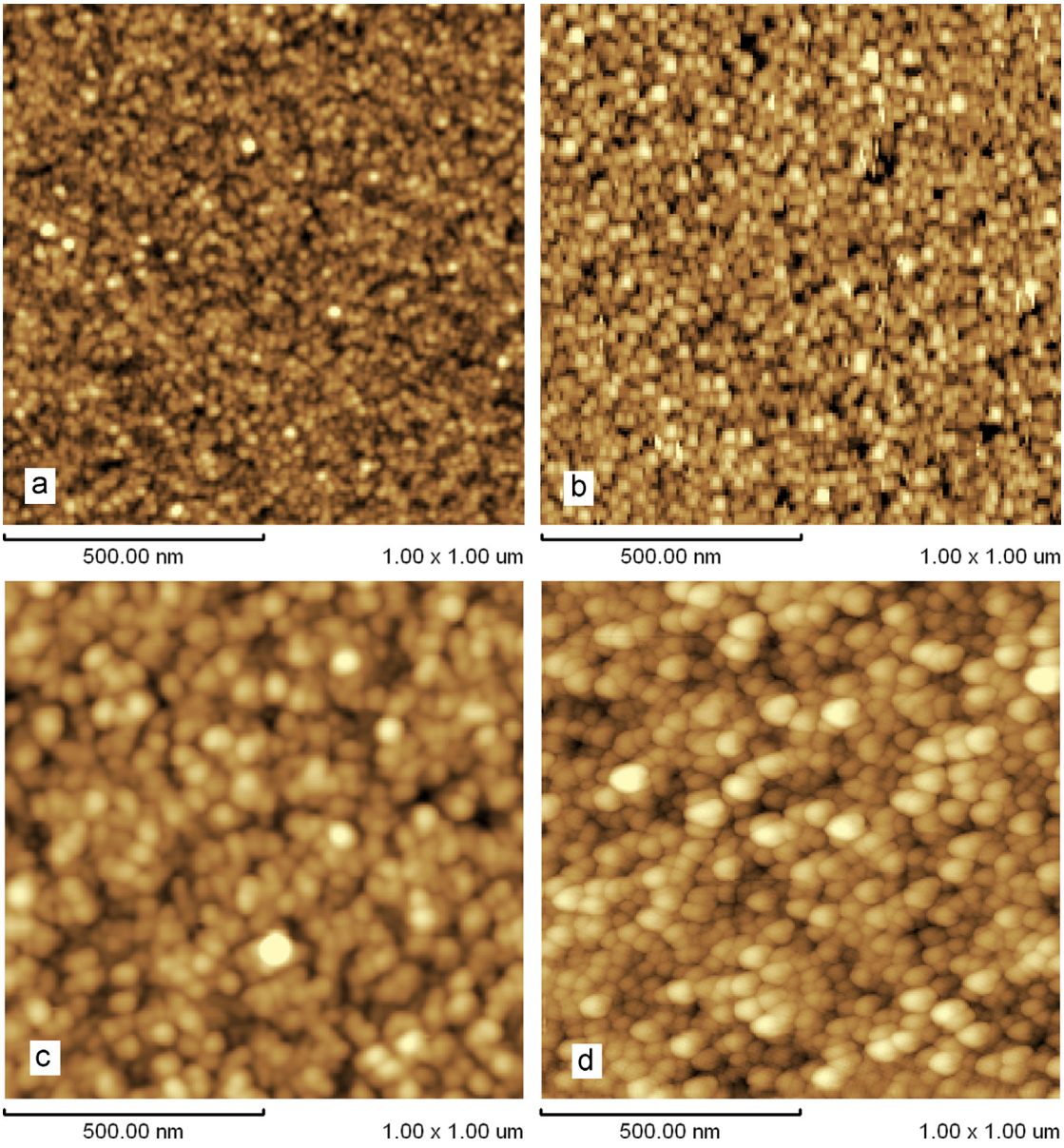

Fig. 6. AFM images of ZnO nanofilms for different Dea:water volume ratios: (a) 16, (b) 8, (c) 4, and (d) 2.

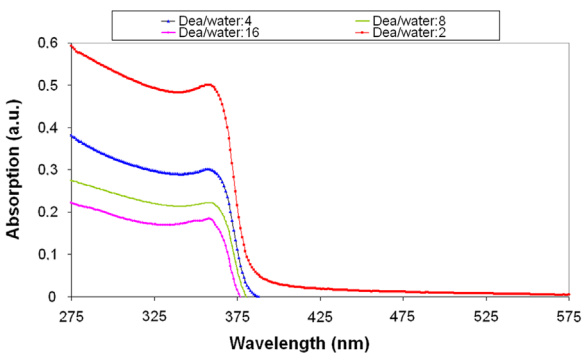

Fig. 7. UV–vis spectra of ZnO nanofilms for different Dea:water volume ratios.

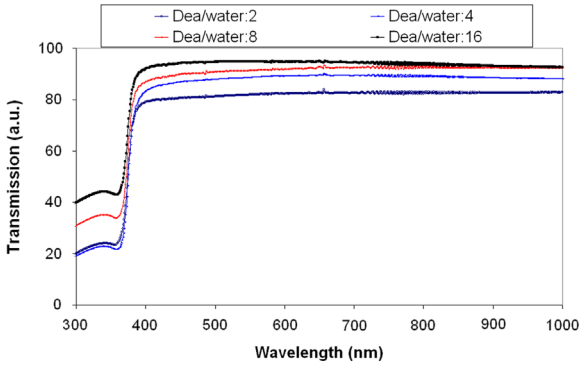

Fig. 8. Transmittance spectra of ZnO nanofilms for different Dea:water volume ratios.

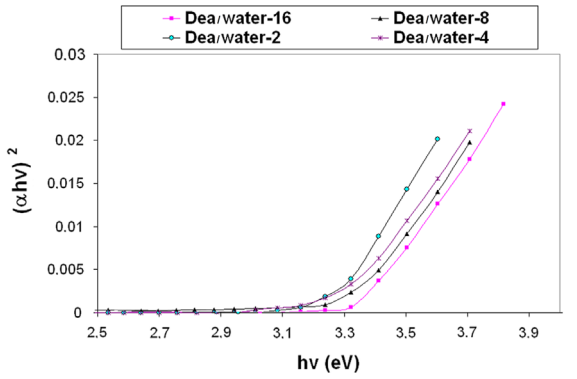

Fig. 9. $(\alpha h\nu)^2$–$h\nu$ graphs of ZnO nanofilms for different Dea:water volume ratios.

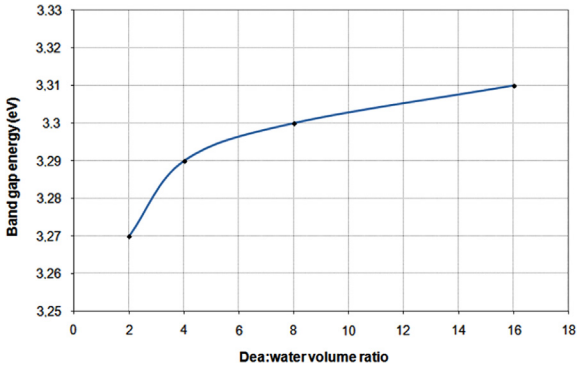

Fig. 10. Plot of band gap energy versus Dea:water volume ratio.

water ratio at the wavelength range from 300 nm to 1000 nm. The optical band gap (E_g) of direct-transitive ZnO thin film can be determined using Tauc's relation [37]

$$\alpha h\nu = A(h\nu - E_g)^{1/2}$$

where α is the linear portion of absorption coefficient, $h\nu$ is the photon energy and A is a constant. Band gap energies of ZnO films are determined to be between 3.31 and 3.27 eV for different Dea:water ratios, as illustrated in Figs. 9 and 10. These values are very close to the band gap of ZnO which have been reported before [38–40]. Band gap energy values of ZnO nanofilms increased with increasing Dea:water ratios.

4. Conclusions

ZnO nanofilms, which were prepared using the sol–gel spin coating method, and the effects of Dea:water ratios on the optical, electrical and structural properties of the film have been investigated. The characteristics of the film depend on the Dea:water ratio. The effect of the Dea: water volume ratio on the crystallinity of film was also investigated. A decrease in the Dea:water ratio leads to the increase in the crystallite size of ZnO films due to the agglomeration. The results indicate that the absorption spectrum shows a red-shift with the increase of Dea:water concentration. Absorption spectrum of ZnO films shifts to a longer wavelength region with the increase of the crystallite size, which decreases the band gap values of films. The activation energy for the particle growth of the films was calculated as 26.3 kJ/mol. The ZnO films with small nanosized particles have a large surface area, and low energy is required for the particle growth of the films. Due to the possibility of controlling the properties easily, ZnO nanofilms can be preferred to be used in electronics and optical applications.

Acknowledgments

The Research Fund of Mimar Sinan University (BAP Project no: 201206) has generously supported this research, and the authors would like to thank Prof. Dr. Fatma Z. Tepehan (ITU Thin Film Laboratory).

References

[1] Z. Neng Ng, K. Chan, T. Tohsophon, Appl. Surf. Sci. 258 (2012) 9604–9609.
[2] M. Popa, R.A. Mereu, M. Filip, M. Gabor, T. Petrisor, L. Ciontea, T. Petrisor, Mater. Lett. 92 (2013) 267–270.
[3] M. Vishwasa, K.N. Rao, A.R. Phani, K.V.A. Gowdad, R.P.S. Chakradhar, Solid State Commun. 152 (2012) 324–327.
[4] C.Y. Tsay, K.S. Fan, Y.W. Wang, C.J. Chang, Y.K. Tseng, C.K. Lin, Ceram. Int. 36 (2010) 1791–1795.
[5] S. Rani, P. Suri, P.K. Shishodia, R.M. Mehra, Sol. Energy Mater. Sol. Cells 92 (2008) 1639–1645.
[6] K.J. Chen, T.H. Fang, F.Y. Hung, L.W. Ji, S.J. Chang, S.J. Young, Y.J. Hsiao, Appl. Surf. Sci. 254 (2008) 5791–5795.
[7] M. Wang, L. Zhang, Mater. Lett. 63 (2009) 301–303.
[8] A. Moballegh, H.R. Shahverdi, R. Aghababazadeh, A.R. Mirhabibi, Surf. Sci. 601 (2007) 2850–2854.
[9] C. Chen, B. Yu, P. Liu, J.F. Liu, L. Wang, J. Ceram. Process. Res. 12 (2011) 420–425.
[10] S. Talam, S.R. Karumuri, N. Gunnam, ISRN Nanotechnol. 372505 (2012) 1–6.
[11] Z. Li, Z. Hu, L. Jiang, H. Huang, F. Liu, X. Zhang, Y. Wang, P. Yin, L. Guo, Appl. Surf. Sci. 258 (2012) 10175–10179.
[12] Y. Ito, O. Sakai, K. Tachibana, Thin Solid Films 518 (2010) 3513–3516.
[13] J.G. Lu, T. Kawaharamura, H. Nishinaka, Y. Kamada, T. Ohshima, S. Fujita, J. Cryst. Growth 299 (2007) 1–10.
[14] P.K. Shishodia, H.J. Kim, A. Wakahara, A. Yoshida, G. Shishodia, R. M. Mehra, J. Non-Cryst. Solids 352 (2006) 2343–2346.
[15] B.M. Ataev, V.V. Mamedov, A.K. Omaev, B.A. Magomedov, Mater. Sci. Semicond. Process. 6 (2003) 535–537.
[16] M. Purica, E. Budianu, E. Rusu, M. Danila, R. Gavrila, Thin Solid Films 403–404 (2002) 485–488.
[17] R. Serhane, S. Abdelli-Messaci, S. Lafane, H. Khales, W. Aouimeur, A. Hassein-Bey, T. Boutkedjirt, Appl. Surf. Sci. 288 (2014) 572–578.
[18] S.-H. Huang, Y.-C. Chou, C.-M. Chou, V.K.S. Hsiao, Appl. Surf. Sci. 266 (2013) 194–198.
[19] R. Khandelwal, A.P. Singh, A. Kapoor, S. Grigorescu, P. Miglietta, N. E. Stankova, A. Perrone, Opt. Laser Technol. 40 (2008) 247–251.
[20] Y. Nakata, T. Okada, M. Maeda, Appl. Surf. Sci. 197–198 (2002) 368–370.
[21] S. Joshi, M.M. Nayak, K. Rajanna, Appl. Surf. Sci. 296 (2014) 169–176.
[22] C. Besleaga, G.E. Stan, A.C. Galca, L. Ion, S. Antohe, Appl. Surf. Sci. 258 (2012) 8819–8824.
[23] V. Tvarozek, I. Novotny, P. Sutta, S. Flickyngerova, K. Schtereva, E. Vavrinsky, Thin Solid Films 515 (2007) 8756–8760.
[24] W. Gao, Z. Li, Ceram. Int. 30 (2004) 1155–1159.
[25] S.-Y. Chu, W. Water, J.-T. Liaw, J. Eur. Ceram. Soc. 23 (2003) 1593–1598.
[26] X. Pan, P. Ding, H. He, J. Huang, B. Lu, H. Zhang, Z. Ye, Opt. Commun. 285 (2012) 4431–4434.
[27] S.P. Wang, C.X. Shan, B. Yao, B.H. Li, J.Y. Zhang, D.X. Zhao, D.Z. Shen, X.W. Fan, Appl. Surf. Sci. 255 (2009) 4913–4915.
[28] Z. Yang, J.-H. Lim, S. Chu, Z. Zuo, J.L. Liu, Appl. Surf. Sci. 255 (2008) 3375–3380.

[29] Y.S. Jung, O.V. Kononenko, W.-K. Choi, Solid State Commun. 137 (2006) 474–477.
[30] S.B. Ran, P. Singh, A.K. Sharma, A.W. Carbonari, R. Dogra, J. Optoelectron. Adv. Mater. 12 (2010) 257–261.
[31] I. Udom, M.K. Ram, E.K. Stefanakos, A.F. Hepp, D.Y. Goswami, Mater. Sci. Semicond. Process. 16 (2013) 2070–2083.
[32] B.D. Cullity, Elements of X-ray Diffraction, Addison-Wesley Publishing Company Inc., London, 1978.
[33] Y.H. Yang, G.W. Yang, Chem. Phys. Lett. 494 (2010) 64–68.
[34] A.A. Vostrikov, O.N. Fedyaeva, A.V. Shishkin, M.Y. Sokol, J. Supercrit. Fluids 48 (2009) 154–160.
[35] S. Danwittayakul, J. Dutta, Chem. Eng. J. 223 (2013) 304–308.
[36] E. Burstein, Phys. Rev. 93 (1954) 632.
[37] J. Tauc, Mater. Res. Bull. 5 (1970) 721.
[38] M.M. Ba-Abbad, A.A.H. Kadhum, A.B. Mohamad, M.S. Takriff, K. Sopian, J. Alloys Compd. 550 (2013) 63–70.
[39] A. Khorsand Zaka, M. Ebrahimizadeh Abrishami, W.H. Abd. Majid, Ramin Yousefic, S.M. Hosseini, Ceram. Int. 37 (2011) 393–398.
[40] Nasrin Talebian, Mohammad Reza Nilforoushan, Najimeh Maleki, Thin Solid Films 527 (2013) 50–58.